Dalton Transactions

PAPER

View Article Online
View Journal | View Issue

Cite this: *Dalton Trans.*, 2016, **45**, 8201

Theoretical insights into the origin of magnetic exchange and magnetic anisotropy in {Re^{IV}–M^{II}} (M = Mn, Fe, Co, Ni and Cu) single chain magnets†

Saurabh Kumar Singh,‡[a] Kuduva R. Vignesh,‡[b] Velloth Archana§[a] and Gopalan Rajaraman*[a]

Density functional calculations have been performed on a series of {Re^{IV}–M^{II}} (M = Mn(**1**), Fe(**2**), Co(**3**), Ni(**4**), Cu(**5**)) complexes to compute the magnetic exchange interaction between the Re^{IV} and M^{II} ions, and understand the mechanism of magnetic coupling in this series. DFT calculations yield *J* values of −5.54 cm^{-1}, +0.44 cm^{-1}, +10.5 cm^{-1}, +4.54 cm^{-1} and +19 cm^{-1} for complexes **1–5** respectively, and these estimates are in general agreement with the experimental reports. Using molecular orbital (MO) and overlap integral analysis, we have established a mechanism of coupling for a {3d–5d} pair and the proposed mechanism rationalises both the sign and the magnitude of *J* values observed in this series. Our proposed mechanism of coupling has five contributing factors: (i) (Re)d_{yz}–d_{yz}(3d) overlap, (ii) (Re)d_{xz}–d_{xz}(3d) overlap, (iii) (Re)d_{xy}–d_{xy}(3d) overlap, (iv) (Re)e_g–t_{2g}(3d) overlaps and (v) (Re)e_g–e_g(3d) overlaps. Here, the first two terms are found to contribute to the antiferromagnetic part of the exchange, while the other three contribute to the ferromagnetic part. The last two terms correspond to the cross-interactions and also contribute to the ferromagnetic part of the exchange. A record high ferromagnetic *J* value observed for the {Re^{IV}–Cu^{II}} pair in complex **5** is found to be due to a significant cross interaction between the d_{z^2} orbital of the Re^{IV} ion and the $d_{x^2-y^2}$ orbital of the Cu(II) ion. Magneto-structural correlations are developed for Re–C and M–N bond lengths and Re–C–N and M–N–C bond angles. Among the developed correlations, the M–N–C bond angle is found to be the most sensitive parameter which influences the sign and strength of *J* values in this series. The *J* values are found to be more positive (or less negative) as the angle increases, indicating stronger ferromagnetic coupling at linear M–N–C angles. Apart from the magnetic exchange interaction, we have also estimated the magnetic anisotropy of $[ReCl_4(CN)_2]^{2-}$ and $[(DMF)_4(CN)M^{II}(CN)]$ (M^{II}–Fe^{II}, Co^{II} and Ni^{II}) units using the state-of-the-art *ab initio* CASSCF/PT2/RASSI-SO/SINGLE_ANISO approach. The calculated *D* and *E* values for these building units are found to be in agreement with the available experimental results. Particularly a large positive *D* computed for the $[ReCl_4(CN)_2]^{2-}$ unit was found to arise from $d_{xz}/d_{yz} \rightarrow d_{xy}$ excitations corresponding to the low-lying doublet states. Similarly, a very large positive *D* value computed for Fe^{II} and Co^{II} units are also rationalised based on the corresponding ground state electronic configurations computed. The non-collinearity of the Re^{IV} ion and the M^{II} ion axial anisotropy (D_{ZZ}) axis are found to diminish the anisotropy of the building unit, leading to the observation of moderate relaxation barriers for these molecules.

Received 18th December 2015,
Accepted 23rd March 2016

DOI: 10.1039/c5dt04928h

www.rsc.org/dalton

Introduction

Since the discovery of single molecule magnet (SMM) Mn_{12} and related clusters, much attention has been paid towards the synthesis and characterization of SMMs.[1–8] SMMs are molecules which show slow relaxation of magnetization for reorientation of the spins in the absence of any applied magnetic field. SMMs have several potential applications ranging from highly dense information storage devices to solid state Q-bits in quantum computing.[1,9] The barrier height for reorientation of magnetization in these clusters is given by the

[a]*Department of Chemistry, Indian Institute of Technology Bombay, Powai, Mumbai-400076, India. E-mail: rajaraman@chem.iitb.ac.in; Fax: +91-22-25767152; Tel: +91-22-25767183*

[b]*IITB-Monash Research Academy, Indian Institute of Technology Bombay, Powai, Mumbai-400076, India*

†Electronic supplementary information (ESI) available. See DOI: 10.1039/c5dt04928h

‡These authors contributed equally to the work.

§Present address: Department of Chemistry, Graduate School of Science and Engineering, Tokyo Metropolitan University, Minami-Osawa 1-1, Hachi-Oji, Tokyo 192-0397, Japan.

spin ground state (S) and the negative axial zero field splitting parameter (zfs; D): $\Delta E = S^2|D|$ (for the integer spin state).[10] Large ground state S values along with large negative zfs are the desired parameters to exhibit slow relaxation of magnetization. In transition metal clusters, the orbital angular momentum is strongly quenched by the ligand field, which generally diminishes the first order contribution to the magnetic anisotropy. The second order contribution to the zfs parameter is of few wave numbers, and decreases significantly with increase in the S value.[11,12] Despite several pioneering studies in transition metal clusters, the barrier height for magnetization reversal has not increased tremendously.[13,14] In view of the fact that attaining large S and D is not a trivial task, another class of one-dimensional chain complexes called single chain magnets (SCMs) has been reported as an alternative to SMMs. Here, the barrier height is given by $\Delta_\tau = (8J + D)S^2$, where the intramolecular exchange interaction J plays a direct role in controlling the barrier heights. As the exchange coupling parameter J is relatively easy to control compared to the zfs parameters, a significant number of one-dimensional chain compounds are reported to behave as SCMs.[15–19] Apart from a strong intrachain magnetic exchange, a negligible interchain exchange interaction is also a requisite for the observance of SCM behaviour.[20–22]

Strategies to incorporate highly anisotropic ions such as heavier congeners of the transition metal ions in the cluster aggregation have become very successful in recent years, as the diffuse 4d and 5d orbitals facilitate stronger magnetic exchange compared to their 3d analogues.[12,23] Besides, the SOC coupling constants in these ions are usually one order higher than their 3d analogues and lead to a highly anisotropic environment, resulting in stabilization of the well isolated ground state doublet from the excited state. The advantage of employing 4d and 5d ions in molecular magnetism has been reported recently by Dunbar and co-workers.[23] The latter transition metal ions with the unquenched orbital angular momentum are more attractive, as they benefitted from both the first order angular momentum and the second order angular momentum. This leads to a strong anisotropic exchange coupling and yields a large anisotropic barrier for magnetization reversal.[24–27] Our detailed theoretical analysis reported earlier reveals that the strength of anisotropic exchange coupling increases as we move down the group, leading to a large barrier for spin reversal.[28]

Generally 4d and 5d metal ions tend to stabilize the higher oxidation states compared to their 3d analogues, and also likely to exhibit a higher coordination number. Besides, these 4d and 5d metal ions are prone to form multiple metal–metal bonds as a result of direct overlap of the frontier orbitals. To avoid the direct metal–metal bonds, cyanide ligands are employed as bridging ligands, and this synthetic strategy leads to isolation of several 4d/5d SCMs.[23] Cyanometalates are very stable in the solution—various oxidation states and spin states can be controlled and the magnetic properties are often predictable.[29–33] In addition, cyanides are a strong-field ligand and preserve the orbital degeneracy of the coordinated metal ions in many cases, which leads to unquenched orbital angular momentum and facilitates anisotropic exchange coupling – another key ingredient in the synthesis of SMMs/SCMs.[34,35]

Recently much attention has been paid to Re^{IV} ion based molecular magnets, and this is evident from the isolation of several SMMs/SCMs based on Re^{IV} building units.[23,31,32,36] The Re^{IV} is a d^3 ion which does not possess any first order orbital angular momentum, but possesses large SOC constants ($\lambda \sim 1000\ cm^{-1}$), and this offers a huge anisotropy, isolating the ground state doublet from the excited state. Particularly, the $[ReCl_4(CN)_2]^{2-}$ unit is a highly anisotropic building block as it has been successfully used to isolate several SCMs with high blocking temperatures for magnetic relaxation.[31] In a seminal report, Long *et al.* reported a series of $[(DMF)_4MReCl_4(CN)_2]$ (where M = Mn^{II}, Fe^{II}, Co^{II}, Ni^{II}) one-dimensional SCMs with thermally activated, energy barriers to relaxation Δ_τ of 31, 56, 17, and 20 cm^{-1} for Mn^{II}, Fe^{II}, Co^{II}, Ni^{II} complexes, respectively.[31] The same group also reported a $(Bu_4N)[TpCuReCl_4(CN)_2]$ complex with a record high ferromagnetic exchange of +29 cm^{-1} between Re^{IV}–CN–Cu^{II} linkage.[37] A recent HF-EPR study on the $[ReCl_4(CN)_2]^{2-}$ unit reveals a positive zfs of +11 cm^{-1} with a large E term affirming our earlier point that these building units possess a significant single-ion anisotropy.[32]

Synthesis of novel 4d/5d SMMs/SCMs demands a thorough understanding and a perceivable way to achieve control of microscopic spin-Hamiltonian parameters. Theoretical tools are invaluable in this area as these molecules possess a complex set of spin Hamiltonian parameters and extracting them using experimental techniques often demands a bunch of sophisticated spectroscopic analyses.[27,29,30,35,38,39] Theoretical methods, on the other hand, help to extract these parameters from the X-ray structure and have also been used lately to make useful predictions.[38,40,41] In the present work, we have studied in detail the mechanism of magnetic exchange interactions of $[(DMF)_4MReCl_4(CN)_2]$ complexes (here M = Mn^{II}, Fe^{II}, Co^{II} and Ni^{II}) by using density functional calculations.[31] Our study also includes the $(Bu_4N)[TpCuReCl_4(CN)_2]$ complex to underpin the factor behind the record high ferromagnetic exchange observed for any cyanometalates.[37] To unearth the source of anisotropy in these systems, we have performed *ab initio* calculations on mononuclear $[ReCl_4(CN)_2]^{2-}$ and $[(DMF)_4(CN)M^{II}(CN)]$ (M^{II} = Fe^{II}, Co^{II} and Ni^{II}) units to compute the zfs parameters. With this data we aim to propose a unified mechanism of magnetic coupling in these systems, and have developed a series of magneto-structural correlations to offer further insight into the nature of magnetic interactions in these series.

Computational details

In dinuclear complexes, the magnetic exchange interaction between the Re^{IV} and M^{II} ions is described by the following Hamiltonian:

$$\hat{H} = -J\hat{S}_M\hat{S}_{Re} \quad (1)$$

The exchange coupling constant is isotropic in nature where S_M and S_{Re} are the spins on M^{II} ions (S_{Mn} = 5/2, S_{Fe} = 2,

$S_{Ni} = 1$, $S_{Cu} = 1/2$) and the spin on Re^{IV}($S = 3/2$). DFT combined with the Broken Symmetry (BS) approach[42] has been employed to compute the energies of the different spin configurations.[43–45] The BS method in conjunction with the equation proposed by Ruiz *et al.*[41,46] has a proven track record of yielding good numerical estimate of J values for a variety of complexes and this has been used throughout our study.[28,38,40,41,46,47] Here, we have performed most of our calculations using Gaussian 09 suite of programs.[48] We have employed a hybrid B3LYP functional along with a relativistic effective-core potential LANL08f basis set on Re atoms. The rest of the atoms are treated with the Ahlrichs ζ triple-zeta basis set.[49] The SCF convergence is kept tight at 1×10^{-8} E_h during the calculations. To analyse the origin of the exchange interactions on Re^{IV}–M^{II} ions, we have replaced the Re^{IV} ion by the Cr^{III} ion, and have computed the Cr^{III}–M^{II} exchange employing the same functional and LANL08f basis set on the Cr atom. The overlap integral was computed as per the procedure outlined in ref. 46. In the case of trinuclear complexes, the magnetic exchange was computed using the pair-wise interaction model,[41] in which four spin-configurations were computed to extract the three different exchange interactions (J_1–J_3) (see the equation below and ESI† for further details). The energy difference between spin configurations is equated to the corresponding pair-wise exchange interaction from which all three J values have been extracted.

$$\hat{H} = -J_1 S_{M_1} S_{Re} - J_2 S_{M_2} S_{Re} - J_3 S_{M_1} S_{M_2} \quad (2)$$

Zero field splitting parameters were computed using the MOLCAS 7.8 code.[50] Here, we have performed state-of-the-art *ab initio* calculations on the mononuclear $[ReCl_4(CN)_2]^{2-}$ unit to extract the zero field splitting of the Re^{IV} ion and on $[(DMF)_4(CN)M^{II}(CN)]$ (M^{II} = Fe^{II}, Co^{II} and Ni^{II}) units to find the D and E values. We have employed the [ANO–RCC⋯8s7p5d3f2g1h] basis set for the Re atom, the [ANO–RCC⋯6s5p3d2f1g] basis set for M^{II} atoms, [ANO–RCC⋯4s3p2d] for C and N atoms, and [ANO–RCC⋯5s4p2d] for Cl atoms. The ground state electronic configuration of the Re^{IV} ion is $5d^3$ with ^4F as the ground state. First, we have performed CASSCF calculations with an active space of three active electrons in the five active 5d orbitals, CAS(3,5). Here, we have computed 10 quartet states and 40 doublets states in the CI procedure. To treat the dynamic correlation, we have performed the MS-CASPT2 calculations on top of the converged CASSCF wavefunctions for the Re^{IV} ion. We have employed IPEA shift of 0.25 to avoid the intruder states problem in CASPT2 calculations. For Fe(II) ions, we have performed CASSCF calculations with an active space of six active electrons in the five active 3d orbitals, CAS(6,5), and then we have computed five quintet states and 45 triplet states in the CI procedure. For Co(II) ions, we have performed CASSCF calculations with an active space of 7 active electrons in the five active 3d orbitals, CAS(7,5) and then computed 10 quartet states and 40 doublet states in the CI procedure. Similarly for Ni(II) ions, we have performed CASSCF calculations with an active space of eight active electrons in the five active 3d orbitals, CAS(8,5) and then computed 10 triplet states and 15 singlet states in the CI procedure. After computing these spin-free states, we have mixed these states in the RASSI-SO module to compute the spin–orbit states. After that, we have taken these states into the SINGLE_ANISO program to compute the zfs parameters.[50] The Cholesky decomposition for two electron integrals is employed with the cut-off value of 1×10^{-3} as recommended earlier.[50] Using the SINGLE_ANISO code, we have also computed the static d.c. properties.[51,52]

Results and discussion

Magnetic exchange interactions in {Re^{IV}–M^{II}} (M = Mn (1), Fe (2), Co (3), Ni (4), Cu (5)) building units

Utilizing $[ReCl_4(CN)_2]^{2-}$ as a basic building unit, synthesis and magnetic studies of $[(DMF)_4(CN)M^{II}(CN)Re^{IV}(Cl)_4(CN)]$ (M = Mn (**1**), Fe (**2**), Co (**3**), and Ni (**4**)) and $[(CN)(Tp)Cu^{II}(CN)Re^{IV}(Cl)_4(CN)]$ (**5**) are reported in the literature (see Fig. 1).[31,37] Here, we have modelled five dinuclear units (repeating units of complexes **1–5**) from the parent chain structure to estimate and to understand the nature of magnetic coupling in these classes of systems. The common building block in these systems is the $[ReCl_4(CN)_2]^{2-}$ unit. Here the Re^{IV} ion possesses an octahedral environment, with four Cl^- ions in the equatorial plane and –CN bridges in the *-trans* position. The average Re–Cl distances are found to be 2.314 Å which is slightly larger than the average Re–CN bond distance of 2.122 Å. This is due to the lack of π acceptance nature of the –Cl ligand compared to the –CN ligand. The *trans* (–CN) ligands are attached to the $M(DMF)_4$ (M = Mn, Fe, Co and Ni; DMF = di-methyl formamide) unit for complexes **1–4** and results in a one-dimensional chain structure. For complex **5**, however, a different topology is detected where {(CN)(Tp)Cu} (here Tp^- is hydrotris(pyrazol-1-yl)borate) is attached to the *trans* –CN ligand of the $[ReCl_4(CN)_2]^{2-}$ unit. The Cu^{II} ion is found to possess a trigonal pyramidal geometry. The selected structural parameters for all the complexes are listed in Table 1.

The experimental magnetic susceptibility measurements for complexes **1–5** yield the following {Re^{IV}–M^{II}} interactions: −5.4 cm^{-1}, +4.8 cm^{-1}, +2.4 cm^{-1}, +3.7 cm^{-1} and +29 cm^{-1}, respectively. The exchange interaction in complex **1** is estimated to be antiferromagnetic in nature while in complexes **2–5**, it is estimated to be ferromagnetic in nature with complex **5** exhibiting a record high exchange coupling reported for any cyanometallate complexes.[53] Among these five complexes, complexes **1–4** are characterised as SCMs with the Δ_τ value of 31, 56, 17, and 20 cm^{-1} respectively. Additionally for complex **1**, the HF-EPR studies have been performed to estimate accurately both the Js and the anisotropic parameters.[32] Complex **5** on the other hand does not exhibit any out-of-phase signals and the zigzag nature of the chain is suggested to be the reason for the absence of the SCM behaviour in this complex.[37]

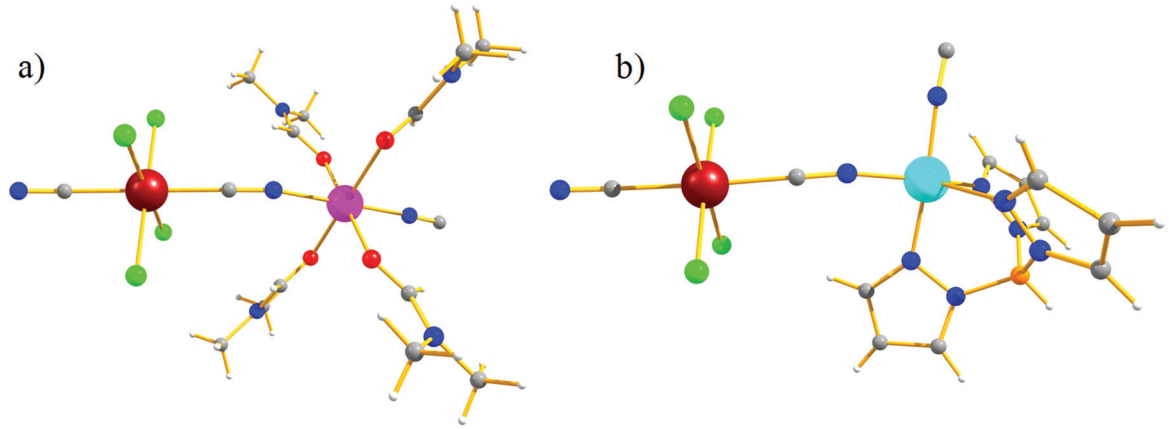

Fig. 1 Representative crystal structures (showing only the dimeric unit) of complexes (a) **1** and (b) **5**. Color code: brown for Re; pink for Mn^{II}; cyan for Cu; light green for Cl; red for O; blue for N; grey for C; and white for hydrogen.

Table 1 Selected X-ray structural parameters of complexes **1–5**

Structural parameters	1	2	3	4	5
Re–C (Å)	2.125	2.118	2.129	2.134	2.111
M–N (Å)	2.228	2.155	2.095	2.111	1.986
M–O (Å)	2.181	2.134	2.099	2.098	
Re–C–N (°)	175.8	175.33	175.95	174.7	175.08
M–N–C (°)	155.8	158.15	160.97	159.4	167.54
Re–Cl (Å)	2.312	2.339	2.338	2.340	2.337

DFT calculations yield the J values of -5.54 cm^{-1}, $+0.44$ cm^{-1}, $+10.5$ cm^{-1}, $+4.54$ cm^{-1} and $+19$ cm^{-1} for complexes **1–5** respectively. The J value in complex **1** is computed to be antiferromagnetic in nature, while in complexes **2–4** it is computed to be ferromagnetic. This trend is in agreement with the experimental results. The magnitude of J values are in agreement with the experimental observations for complexes **1** and **4**, while it deviates for complexes **2** and **3**. This may be attributed to the anisotropic nature of Fe^{II} and Co^{II} metal ions, which were further confirmed by *ab initio* calculations (*vide infra*). Complex **5** is found to possess a very large ferromagnetic interaction, although the magnitude is underestimated – our calculations reveal that the $\{Re^{IV}$–$Cu^{II}\}$ exchange present in complex **5** is very strong.

As the ground state for complexes **1–5** are correctly reproduced, this has allowed us to analyse the mechanism of magnetic coupling in this class of complexes. The net magnetic exchange J has two contributions: J_F arises essentially due to orthogonality of the magnetic orbitals while J_{AF} arises due to the overlap of magnetic orbitals. Thus analysis of the overlap integral values and the spin density is likely to help in elucidating the mechanism of magnetic coupling in **1–5**.

The electronic configuration of the Re^{IV} ion is computed to be $(d_{xy})^1(d_{xz})^1(d_{yz})^1(d_{z^2})^0(d_{x^2-y^2})^0$ and this is similar to its 3d congener Cr^{III} ion. The d_{xz} and d_{yz} orbitals are of π-type and actively involved in electron delocalisation *via* π* orbitals of the –CN ligand to the next attached partner and contribute significantly to the J_{AF} part of the exchange. The unpaired electron in the d_{xy} orbital on the other hand is δ type in nature and generally contributes to the ferromagnetic part of the exchange[28] (see Scheme 1).

The contributions to the net exchange are analysed *via* the overlap integrals and the following equation describes the nature of magnetic exchange in complex **1**.

$$J_{net} = J_{AF}\overbrace{\left[Mn(d_{yz})^1 - Re(d_{yz})^1\right]}^{\text{term I}} + J_{AF}\overbrace{\left[Mn(d_{xz})^1 - Re(d_{xz})^1\right]}^{\text{term II}} + J_F\overbrace{\left[Mn(d_{xy})^1 - Re(d_{xy})^1\right]}^{\text{term III}} + J_{F(cross)}\underbrace{\left[Mn(d_{xz})^1/(d_{yz})^1/(d_{xy})^1 - Re(d_{z^2})^0/(d_{x^2-y^2})^0\right]}_{\text{term IV}} + J_{F(cross)}\underbrace{\left[Mn(d_{z^2})^1/(d_{x^2-y^2})^1 - Re(d_{z^2})^0/(d_{x^2-y^2})^0\right]}_{\text{term V}} \quad (3)$$

Here the first two interactions (terms I and II) contribute significantly to the J_{AF} term where the $3d(d_{yz})$–$5d(d_{yz})$ and $3d(d_{xz})$–$5d(d_{xz})$ overlap integrals are important. Although both overlaps are expected to be the same when the Re–C–N and C–N–M bond angles are linear, the nature of overlap is expected to be different when these angles are different. As shown in Table 1, the Re–C–N bond angle is close to linearity in all cases, while the C–N–M bond angle is acute. This bending does not influence the nature of $3(d_{yz})$–$5d(d_{yz})$ overlap but significantly influences the $3d(d_{xz})^1$–$5d(d_{xz})^1$ overlap as shown in Scheme 1. The third interaction $3(d_{xy})$–$5d(d_{xy})$ overlap is δ-type in nature and contributes to the J_F term. The term IV describes the interaction between the t_{2g} orbitals of the Re^{IV} ion and the e_g orbital of 3d metal ions, and this is expected to contribute to the J_F term. The last term (V) corresponds to the cross interaction where an overlap between the empty orbital of the Re^{IV} ion and singly occupied e_g orbitals of the 3d elements is expected, and this also contributes to the J_F term.[54–56] Unlike

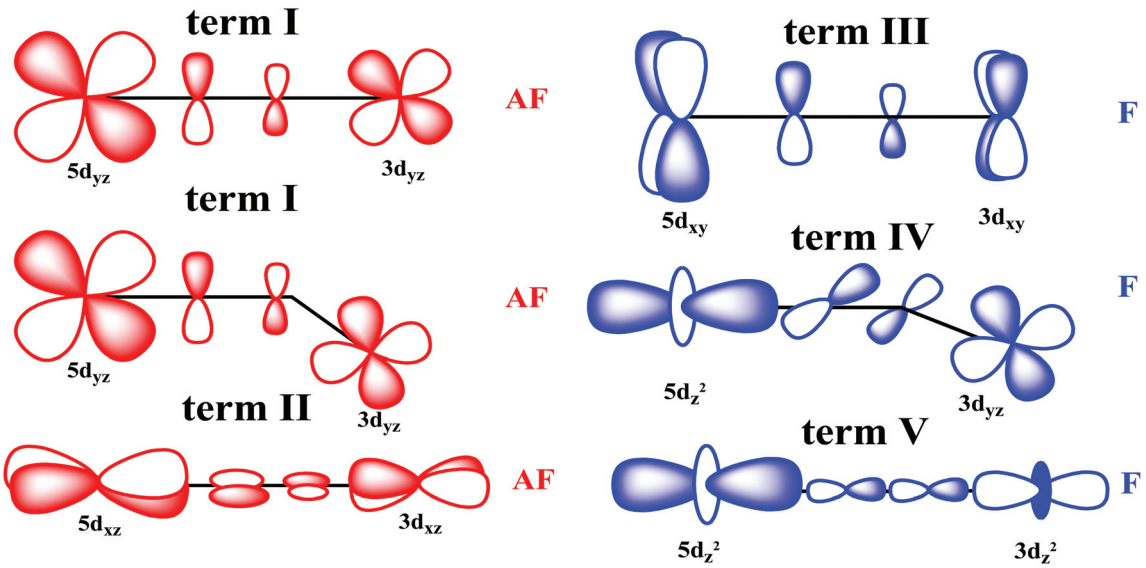

Scheme 1 Schematic representation of dominant orbital interactions present in the M–NC–Re complexes of **1–4**. See eqn (3) for the description of terms I–V.

the other interactions, the cross interaction does not contribute directly to the exchange coupling. These interactions occur between the ground and excited states configurations where an electron has been transferred from a singly occupied molecular orbital (SOMO) centred on one metal into a virtual molecular orbital (VMO) on the other site. The contributions from this term are correlated to the strength overlap integrals between the SOMO–VMO pairs with larger overlaps leading to more pronounced contributions to the J_F term.

In the case of complex **1**, the Mn^{II} ion has the $t_{2g}^3e_g^2$ electronic configuration and this interacts with $t_{2g}^3e_g^0$ set orbitals of the Re^{IV} ion. Here, terms I and II are expected to be dominant, however a smaller C–N–M angle (155.8°) significantly diminishes the overlap between the d_{xz} orbitals (term II), leading to a weak antiferromagnetic coupling. Although all the other contributions are ferromagnetic, terms I and II critically determine the sign of coupling as they contribute significantly to the net exchange interactions. This is supported by the computed overlap integrals (see Table ST1 in the ESI†).

For complex **2**, the Fe^{II} ion is detected to have the following ground state configurations, $(d_{yz})^2(d_{xy})^1(d_{xz})^1(d_{x^2-y^2})^1(d_{z^2})^1$ from our DFT calculations. The following equation is applicable in this scenario,

$$J_{net} = J_{AF}\overbrace{\left[Fe(d_{xz})^1 - Re(d_{xz})^1\right]}^{\text{term II}} + J_F\overbrace{\left[Fe(d_{xy})^1 - Re(d_{xy})^1\right]}^{\text{term III}} + J_{F(cross)}\overbrace{\left[Fe(d_{xz})^1/(d_{xy})^1 - Re(d_{z^2})^0/(d_{x^2-y^2})^0\right]}^{\text{term IV}} + J_{F(cross)}\underbrace{\left[Fe(d_{z^2})^1/(d_{x^2-y^2})^1 - Re(d_{z^2})^0/(d_{x^2-y^2})^0\right]}_{\text{term V}} \quad (4)$$

Here as the d_{yz} orbital is doubly occupied and therefore term I which contributes significantly to the J_{AF} part in complex **1** vanishes. Although term II is still present, the C–N–M angle is also acute here (158.2°) leading to a weaker overlap. As the terms III–V contribute to the ferromagnetic coupling, this leads to an overall small ferromagnetic coupling for this complex (see Table ST2 in the ESI†).

For complex **3**, the Co^{II} ion is detected to have the following ground state configurations, $(d_{yz})^2(d_{xy})^2(d_{xz})^1(d_{z^2})^1(d_{x^2-y^2})^1$ from our DFT calculations. The following equation is applicable in this scenario,

$$J_{net} = J_{AF}\overbrace{\left[Co(d_{xz})^1 - Re(d_{xz})^1\right]}^{\text{term II}} + J_{F(cross)}\overbrace{\left[Co(d_{xz})^1 - Re(d_{z^2})^0/(d_{x^2-y^2})^0\right]}^{\text{term IV}} + J_{F(cross)}\underbrace{\left[Co(d_{z^2})^1/(d_{x^2-y^2})^1 - Re(d_{z^2})^0/(d_{x^2-y^2})^0\right]}_{\text{term V}} \quad (5)$$

Here as both the d_{yz} and d_{xy} orbitals are doubly occupied, hence both terms I and III, where earlier term offers dominant J_{AF} contribution while latter offers weak J_F contributions are vanished, leading to overall ferromagnetic exchange contribution (see Table ST3 in the ESI†). We would like to note here that for complexes **2** and **3**, due to the presence of a residual angular momentum, the exchange interaction is expected to be anisotropic in nature. However here we have assumed this to be isotropic to qualitatively analyse the trend as we move along the first row transition metal series.

For complex **4**, the Ni^{II} ion has the following electronic configuration $(d_{yz})^2(d_{xz})^2(d_{xy})^2(d_{z^2})^1(d_{x^2-y^2})^1$. The following equation is applicable in this scenario,

$$J_{net} = J_{F(cross)}\overbrace{\left[Ni(d_{z^2})^1/(d_{x^2-y^2})^1 - Re(d_{z^2})^0/(d_{x^2-y^2})^0\right]}^{\text{term V}} \quad (6)$$

Here terms I, II, III and IV are vanished and only V contributes to ferromagnetic coupling (see Table ST4 in the ESI†). This leads to a moderate ferromagnetic coupling in this complex.

In complex **5**, the unpaired electron is present in the $d_{x^2-y^2}$ orbital, and thus terms I, II and III are vanished and the main contributing factor is term V leading to a ferromagnetic coupling. The following equation is applicable in this scenario,

$$J_{net} = J_{F(cross)} \overbrace{[Cu(d_{x^2-y^2})^1 - Re(d_{z^2})^0]}^{\text{term V}} \quad (7)$$

As the structural topology here is different compared to complexes **1–4**, there are some significant changes in the structural parameters. Particularly the C–N–Cu angle is found to 167.5° and this is *ca.* 8° larger than that observed for other complexes. Additionally due to Jahn–Teller distortions, the Cu–N bond distances are relatively shorter (Jahn–Teller compressed axis at a Cu–N distance of 1.986 Å, see Table 1) compared to other complexes. These two structural parameters are found to promote the cross interactions (term V) significantly in complex **5** compared to other complexes. Particularly a significant interaction between the $Cu(d_{x^2-y^2})$ and $Re(d_{z^2})$ is detected (see Table ST5 in the ESI† for computed overlap integral values), and this interaction enhances the magnitude of ferromagnetic coupling significantly (see Fig. 2).

One of the primary reasons for the strong ferromagnetic exchange observed in this series is due to the cross interaction which stems from the fact that the Re^{IV} ion possesses unpaired electrons in the 5d orbitals which are large and are diffuse in nature compared to its 3d congener. To affirm this point, we have performed calculations on $\{Cr^{III}–Mn^{II}(\mathbf{1a})/Cu^{II}(\mathbf{5a})\}$ models using structures of complexes **1** and **5** without altering any structural parameters. This yields a J value of -9.6 cm^{-1} for **1a** and $+9.0$ cm^{-1} for **5a**. The antiferromagnetic interaction

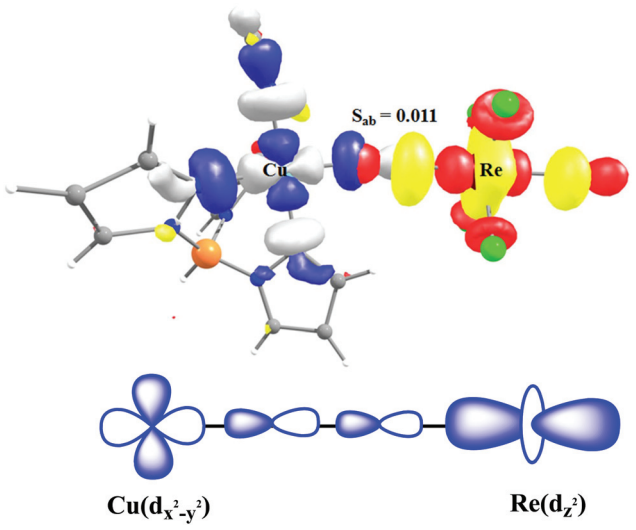

Fig. 2 The representative magnetic orbitals of $Cu(d_{x^2-y^2})$ and $Re(d_{z^2})$ with an overlap value of 0.011. The isodensity surface represented here corresponds to a value of 0.036 e^- $bohr^{-3}$ (top). The schematic illustration of orbital interaction corresponding to complex **5**.

computed for **1a** is ~50% higher while the ferromagnetic interaction in **5a** is ~50% lower compared to the parent structures. This is essentially due to the fact that the cross interaction with the $Cr(d_{z^2})$ and $3d(d_{x^2-y^2})$ orbitals is much weaker compared to the Re^{IV} ion leading to a significant drop in the contribution arising from term V in both cases. This illustrates the importance of the cross interaction and the presence of 5d orbitals in mediating the magnetic exchange interaction.

To gain further insights into the mechanism of magnetic coupling, we have analysed the spin densities on the complexes **1–5** (see Fig. 3). The spin densities on the M^{II} metal ions are computed to be 4.81, 3.79, 2.77, 1.74 and 0.64 for complexes **1–5** respectively. All the M^{II} ions possess spin densities less than those expected based on the number of unpaired electrons and this reveals significant spin delocalization. This is essentially due to the fact that generally electrons in the t_{2g} orbitals promote spin polarization while electrons in the e_g orbitals promote delocalization, with the latter being predominant if unpaired electrons are present in both sets of orbitals.[57] The Re^{IV} ion, on the other hand, has a spin density of ~2.4 in all the complexes and this reflects a significant spin delocalization by this ion. A closer look at the spin density plot reveals that it promotes spin polarization along the –CN bridge and delocalization along the –Cl ligands. This is contrary to the behaviour expected for a d^3 ion where spin polarization is expected to be the only mechanism of coupling (note that in models **1a** and **5a** the Cr^{III} ions possess spin density of ~3.04). However, the large and diffuse nature of the 5d orbitals promote strong delocalization of unpaired electrons to the –Cl ligands (~0.11 to 0.13 spin density is detected) while the vacant d_{z^2} orbital which lies along the –CN ligands promotes spin polarization. This mixture of mechanisms detected further illustrates the importance of cross interaction present in these complexes.

In addition to this, the –N atom of the bridging cyanide ligands is found to contain positive spin densities in all cases. The magnitude of the spin density on this nitrogen atom is found to increase in the following order: **1** < **2** < **3–4** < **5**. The ferromagnetic contribution to the J values is computed to follow the same trend (see Tables ST6–ST10 in the ESI†).

As the reported complexes are one-dimensional chains, beyond the $\{Re^{IV}–M^{II}\}$ interactions, there are also possible (1,3) next-nearest-neighbour $M^{II}–M^{II}$ interactions present in these complexes. Besides, the presence of additional M^{II} units on the Re^{IV} unit could also influence the computed $\{Re^{IV}–M^{II}\}$ interactions. We have earlier studied in detail the magnetic exchange interaction in {3d–4f–3d} complexes and established the importance of (1,3) interactions in these clusters.[47,58] To probe these effects here, we have modelled a $[(CN)(Tp)Cu^{II}(CN)Re^{IV}(Cl)_4(CN)Cu^{II}(CN)(Tp)]$ (model **5b**; Fig. 4a) complex from the X-ray structure of complex **5** as a representative example. We have modelled three different interactions as the structural parameters describing slightly different $\{Cu^{II}–Re^{IV}\}$ and $\{Re^{IV}–Cu^{II}\}$ interactions (see Fig. 4a). The J_1 and J_2 interactions represent $\{Re^{IV}–Cu^{II}\}$ interactions while the J_3 interaction corresponds to the (1,3) $\{Cu^{II}–Cu^{II}\}$ interaction. The J_1–J_3 interactions

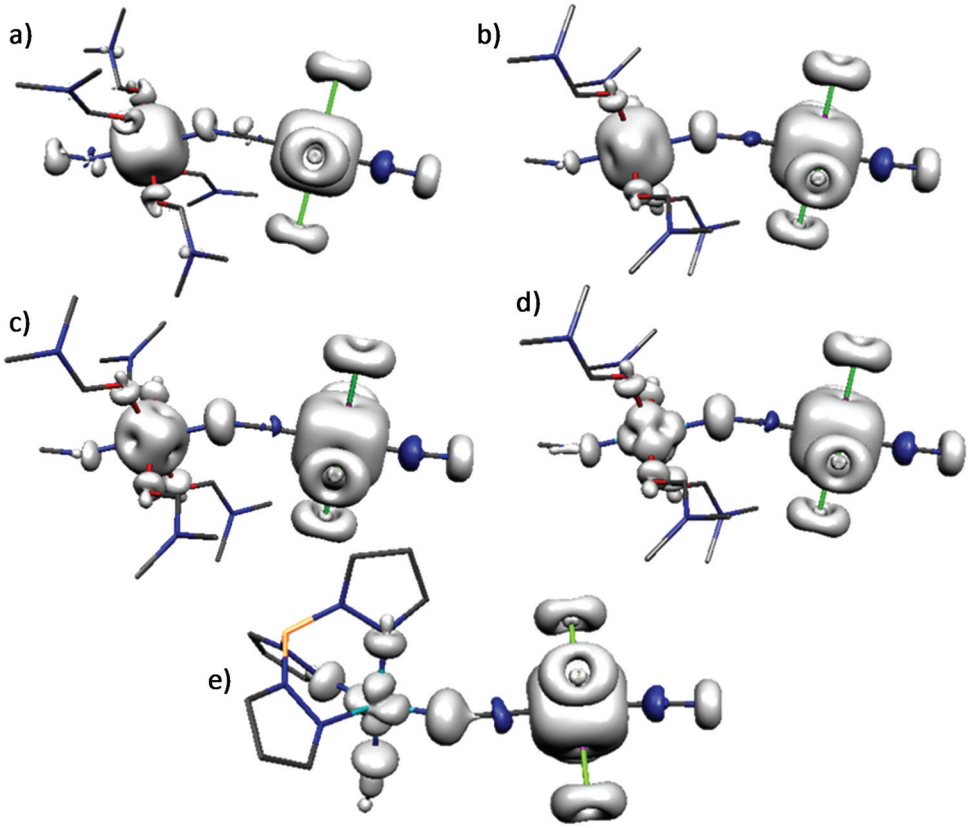

Fig. 3 DFT computed spin-density plot for (a) **1** with the S = 4 state; (b) **2** with the S = 7/2 state; (c) for **3** with the S = 3 state; (d) for **4** with the S = 5/2 state; (e) for **5** with the S = 2 state. The isodensity represented here corresponds to a cut-off value of 0.005 e^{-} $bohr^{-3}$. The white and blue regions indicate the positive and negative spin densities respectively.

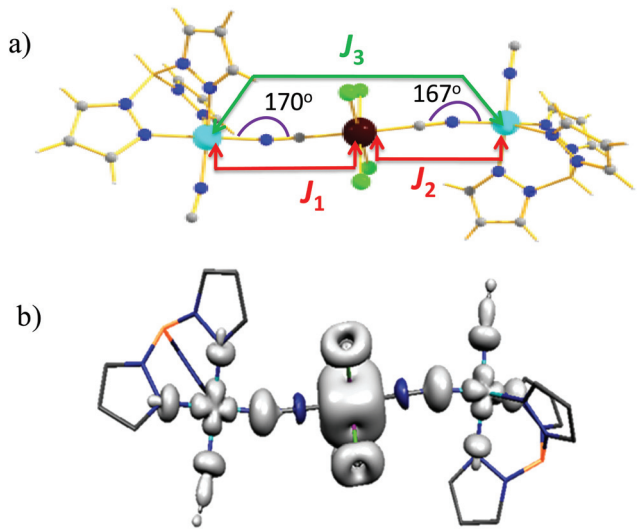

Fig. 4 (a) Trinuclear model of complex **5b** along with the exchange pathways in the complex; (b) DFT computed spin density for the S = 5/2 state. The isodensity represented here corresponds to a cut off value of 0.005 e^{-} $bohr^{-3}$. The white and blue regions indicate the positive and negative spin densities respectively.

are estimated to be +19.0 cm^{-1}, +18.5 and −0.7 cm^{-1} respectively (see Table ST11 and Scheme S1 in the ESI† for details on fitting). Here both J_1 and J_2 interactions are computed to be ferromagnetic and this suggests that the larger model seems to have a negligible effect on the {Re^{IV}–Cu^{II}} interactions estimated on the dinuclear model. The J_3 interaction is found to be antiferromagnetic in nature but its magnitude is substantially smaller compared to the {Re^{IV}–Cu^{II}} interactions. This suggests that (1,3) next-nearest-neighbour interactions can be ignored in this class of complexes for modelling the magnetic susceptibility data. The computed spin density for Cu^{II} and Re^{IV} is very similar to that of dinuclear models and this affirms the proposed mechanistic point of view (Fig. 4b).

Magneto-structural correlations

The magneto-structural correlations are an important means to interpret the observed magnetic properties of novel compounds in order to design new compounds with the expected magnetic properties. To ascertain the influence of different structural parameters on the computed J values, we have developed magneto-structural correlations on complexes **1** and **5**. Four structural parameters are likely to influence the magnetic exchange interactions in these complexes: they are Re–C and Cu^{II}/Mn^{II}–N distances, Re–C–N and Cu^{II}/Mn^{II}–N–C bond angles.

Magneto-structural correlations for Re–C bond distances. The Re–C bond lengths in complexes **1** and **5** are 2.125 Å and 2.111 Å respectively. Moreover, the Re–C distance is found to vary from 2.0 to 2.6 Å in the reported Re^{IV} ion complexes.[31,32,36,37] Keeping this in mind, we have varied the Re–C distance from 1.7 to 2.3 Å on models **1** and **5** without altering any other structural parameters. The magnitude of the *J* value is found to correlate with the distance by an exponential function (see Table ST12 in the ESI† for details on fitting) for both complexes. However the observed trend for **1** and **5** contradict each other (Fig. 5a). For complex **1**, decreasing the Re–C distance from 2.3 Å increases the antiferromagnetic coupling with strong antiferromagnetic *J*s noted at shorter Re–C distances. On the other hand, decreasing the Re–C distance from 2.4 Å increases the ferromagnetic coupling with strong ferromagnetic *J*s noted at shorter Re–C distances for complex **5** (see Table ST13 in the ESI† for details). As longer distances are found to yield *J* which is close to zero, we have restricted our correlations to a Re–C distance of 2.3 Å. For complex **1**, decreasing the Re–C distance would significantly enhance the contributions from terms I and II leading to a stronger antiferromagnetic coupling, while in complex **5** the cross interaction (term V) is expected to be stronger at shorter distances leading to a very strong ferromagnetic coupling of +80 cm^{-1} at a very short Re–C distance. The computed overlap integral affirms this point (see Table ST14 in the ESI†). Although the Re–C bond distances significantly affect the *J* values for both complexes **1** and **5**, switching of the sign of *J* values is not detected in both cases. Besides, given the fact that the Re–C distances are very similar for complexes **1–5**, this parameter is unlikely to be the decisive structural parameter for altering the exchange coupling in this series.

Magneto-structural correlations for Mn/Cu–N bond distances. The second magneto-structural correlation is developed by varying the Mn/Cu–N distances, and, here as well, the computed *J* values are correlated to the distance by an exponential function (see Fig. 5b, see Table ST15 in the ESI† for details). The M–N distances are found to significantly vary among the structures from 2.23 to 1.99 Å. This suggests that this distance could in fact be altered by the structural variations. The observed correlation is very similar to that of the Re–C distance correlation. As decreasing the Mn–N distance from 2.4 Å is found to increase the antiferromagnetic coupling while decreasing the Cu–N distance enhances the ferromagnetic coupling. The strength of antiferromagnetic coupling at the shortest Mn–N distance is found to be stronger than that observed for the corresponding Re–C distance but when it comes to ferromagnetic coupling, the Re–C distance is found to be dominant over the Cu–N distance.

Magneto-structural correlations for the Re–C–N bond angle. Although this parameter is very rigid as this bond angle is found to be very close to ~175° in all five complexes, we have

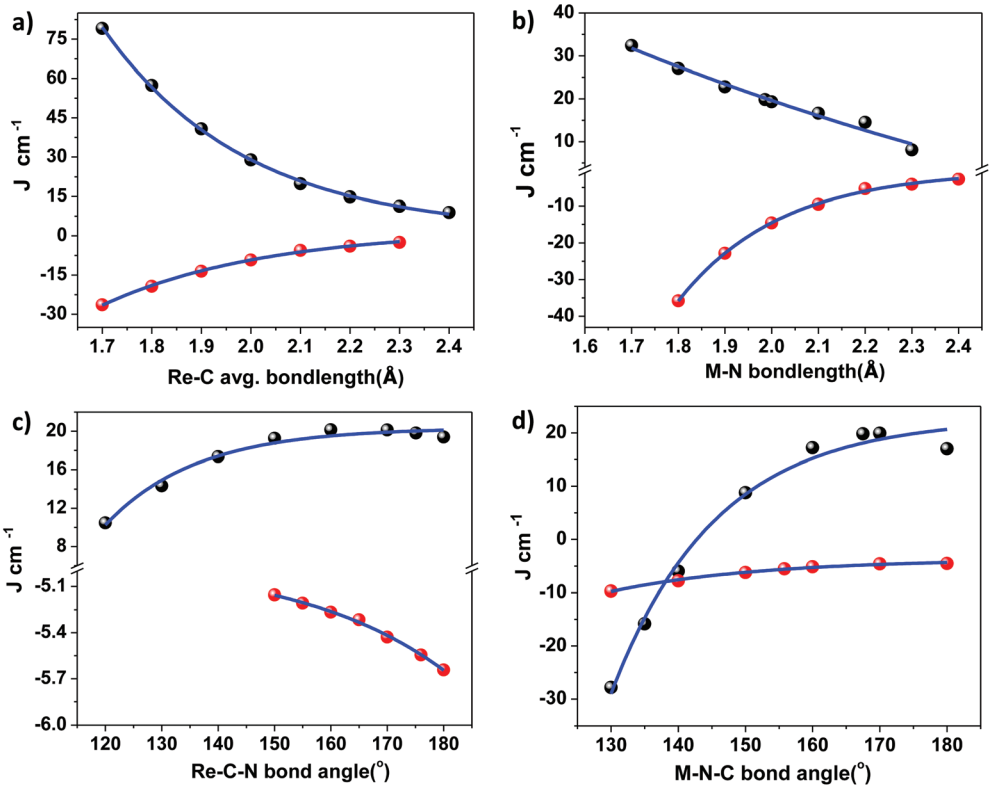

Fig. 5 Magneto-structural correlations developed by DFT calculations for complexes **1** and **5** by varying different structural parameters. (a) Re–C bond distance, (b) M–N bond distance, (c) Re–C–N bond angle, and (d) M–N–C bond angle. The red circle points correspond to complex **1** and the black circle points correspond to complex **5** values. The blue lines are the best fit to the points.

developed a correlation to gain its influence on the J values. The correlation developed by varying the bond angle from 150° to 180° in **1** and from 120° to 180° in **5** is shown in Fig. 5c. Decreasing the bond angle is found to decrease the J value for both the complexes; however the variation observed in J values is relatively small compared to other correlations developed (see Table ST16 in the ESI† for details on fitting).

Magneto-structural correlations for the M–N–C bond angle. The fourth correlation is developed by varying the M–N–C bond angle from 130° to 180°. This angle is also found to be flexible as it is found to vary from 155° to 167° among the complexes **1–5**. Variants of complex **2**, with different coordinating solvents were synthesized and characterized by Long *et al.*, earlier when the C–N–Fe angle was found to vary from 154° to 180°.[36] For these structures, the $\{Re^{IV}–Fe^{II}\}$ J values are estimated to vary from +4.2 cm^{-1} to +7.2 cm^{-1} with a larger angle yielding a stronger ferromagnetic coupling. Here, we have developed a correlation for complexes **1** and **5** and the developed correlation is shown in Fig. 5d. Here, the J value is found to vary exponentially with respect to the bond angle (see Table ST17 in the ESI† for details), and decreasing the bond angle is found to increase the J_{AF} contributions to the J value, thus leading to strong antiferromagnetic couplings at acute angles for both the complexes **1** and **5**. This is in agreement with the experimental correlation established for the $\{Re^{IV}–Fe^{II}\}$ complex.[36]

Interestingly for complex **5**, a switch in the sign of the J value has been noted. At smaller Cu–N–C angles, the term II (angle dependent overlap) is expected to gain strength leading to larger negative J values. Besides, at these angles, the cross interaction between $Cu(d_{x^2-y^2})$ and $Re(d_{z^2})$ is also expected to decrease, leading to a significant decrease in the ferromagnetic contributions. Furthermore, at very acute angles, the $d_{x^2-y^2}$ orbital begins to overlap with the d_{yz}/d_{xz} orbitals leading to dominant antiferromagnetic contributions. This leads to a net strong antiferromagnetic coupling at lower angles (see overlap integrals in Tables ST18 and ST19 of the ESI†).

Since this correlation is found to be the most important one among all the structural parameters studied, we have further developed this correlation for complexes **2** and **4** (see Fig. 6a and b). The correlation developed by varying the Ni/Fe–N–C angle reveals a similar trend where a larger angle is found to yield a stronger ferromagnetic coupling. The experimental points taken from the reported structures and along with the experimental Js are superimposed in our developed correlation[36] (pink circles in Fig. 6a) and the trend observed here is the same as that of the correlation computed using DFT calculations. This offers confidence on our computed correlation. The deviation found between the experimental and theoretical points could be attributed to the fact that in the experimental structures reported apart from the Fe–N–C bond angle, the Fe–N bond distance also alters significantly (varies from 2.174 Å to 2.075 Å). Our developed magneto-structural correlations suggest that the bond angle is the most sensitive parameter to control the sign as well as the magnitude of the magnetic exchange in this class of complexes. This suggests that enhancing the Cu–N–C angle beyond 165° is likely to increase the ferromagnetic coupling further.

Magnetic anisotropy of $[ReCl_4(CN)_2]^{2-}$ and $[(DMF)_4(CN)M^{II}(CN)]$ units

Complexes **1–4** were found to exhibit slow relaxation of magnetization, irrespective of the nature of magnetic coupling. However complex **5** does not exhibit an SMM characteristic as the chains are found to be zigzag in nature, cancelling the overall magnetic anisotropy.[37] In complexes **1–5**, the one source of anisotropy is the $[ReCl_4(CN)_2]^{2-}$ unit while the second source is the $[(DMF)_4(CN)M^{II}(CN)]$ unit for complexes **2–4**. The Mn^{II} ion present in complex **1** is generally isotropic in nature while the Cu^{II} ion in complex **5** does not possess any single-ion anisotropy. To analyse in detail the magnetic anisotropy of these mononuclear building blocks, we have performed CASSCF/PT2/RASSI-SO calculations on the monomeric model complexes.

Magnetic anisotropy of the $[ReCl_4(CN)_2]^{2-}$ unit. The Re^{IV} ions are highly anisotropic in nature due to very large spin–orbit interactions ($\lambda \sim 1000$ cm^{-1}). In general due to the large SOC of the Re^{IV} unit, the ground state of Re^{IV} ions becomes

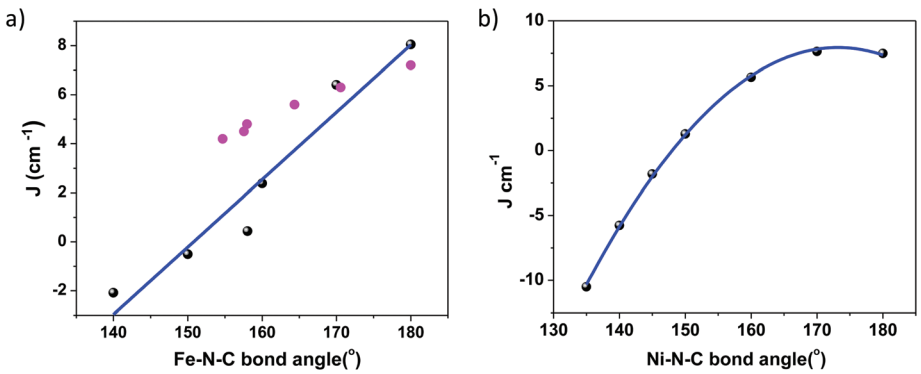

Fig. 6 Magneto-structural correlations developed by DFT calculations for complexes (a) **2** and (b) **4** by varying the Fe/Ni–N–C bond angle. The pink circle points correspond to the experimental structures and exchange values; the black circle points correspond to the computed values. The blue lines correspond to the best fit for the data points.

highly anisotropic and well separated from the excited states, which results in a very large axial zero-field splitting parameter *D*. The experimental HF-EPR on the mononuclear $(NBu_4)_2[ReCl_4(CN)_2]$ complex yields a positive zero field splitting of +11 cm^{-1}.[32] The six coordinated Re^{IV} ion has a ^4F ground state and this further splits into $^4A_2$, $^4T_1$ and $^4T_2$ states under an octahedral environment. The MS-CASPT2 computed *D* value is found to be +16.06 cm^{-1} for the $[ReCl_4(CN)_2]^{2-}$ unit, and this is in good agreement with the HF-EPR measurements (see Table ST20† for details).[32] The computed orientation of the *D*-tensor is shown in Fig. 7a, where the D_{zz} axis is pointed towards the direction of the axial –CN ligand with a tilt of 30.1°. The computed magnetic susceptibility of this mononuclear unit correlates well with the experiments and offers confidence on the estimated anisotropy parameter (see Fig. 7b).

The computed spin-free states suggest that the doublet states are the low-lying excited states, and are expected to contribute significantly to the *D* values.[59] It is important to note here that the second order perturbation has a very strong impact on the low-lying excited states, especially the doublet states which become closer to the ground state in comparison with the CASSCF states (see Fig. 8a). To understand the origin behind the positive zfs observed in this unit, we have analysed the MO orbitals (see Fig. 8b).

The transition from the d_{xy} to $d_{x^2-y^2}$ orbital is spin-allowed and contributes to the negative *D* value as this transition is between the same $|\pm m_l|$ levels. A very small gap has been encountered between the (d_{xz}, d_{yz}) orbitals and the d_{xy} orbital, and this spin–flip excitation from the $d_{xz}/d_{yz} \rightarrow d_{xy}$ orbital contributes to the $|D_{XX}|$ and $|D_{YY}|$ components leading to a positive contribution to the *D* value.

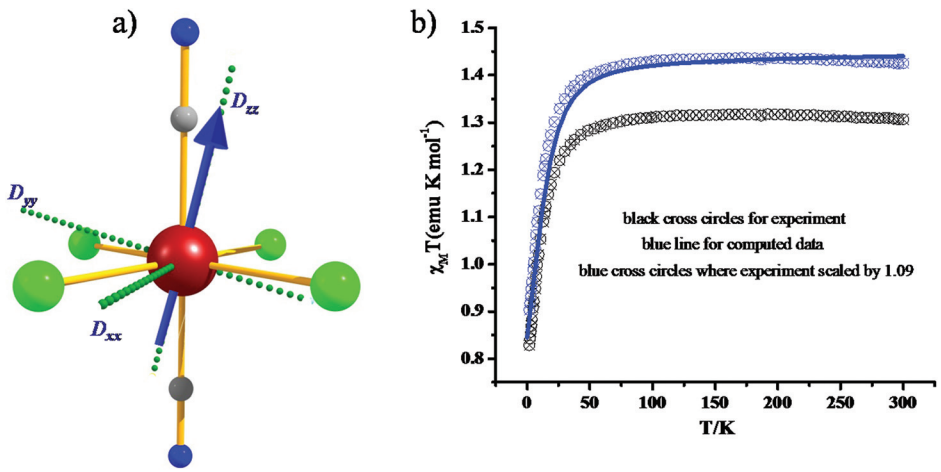

Fig. 7 (a) X-ray structure of the $[ReCl_4(CN)_2]^{2-}$ unit along with the *ab initio* computed *D*-tensor orientations; (b) experimental and computed magnetic susceptibility. The experimental data plotted are obtained from ref. 32.

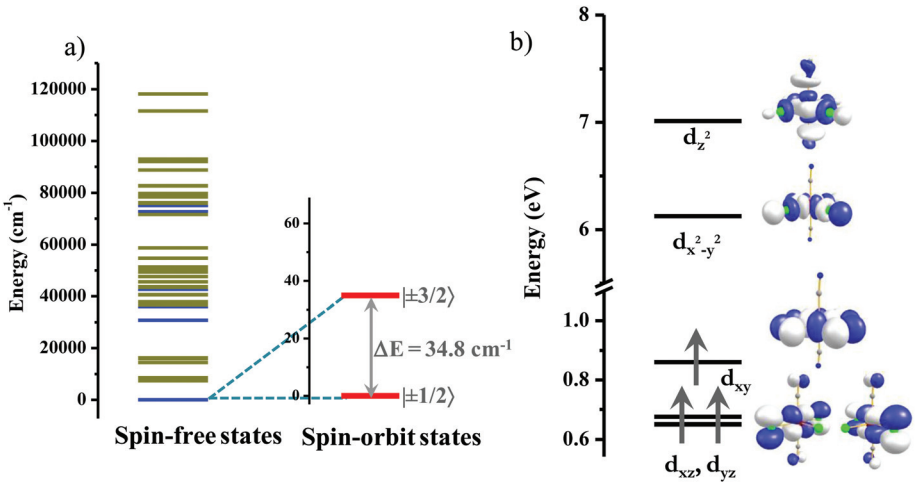

Fig. 8 (a) CASSPT2 + RASSI computed spin-free states and spin–orbit states. The blue thick lines show the computed quartet states while dark yellow lines represent computed doublet states. The red lines represent the first two Kramers doublets. (b) Crystal field splitting pattern of d-orbitals of the Re(IV) ion in the same.

Magnetic anisotropy of the $[(DMF)_4(CN)M^{II}(CN)]$ (M^{II}–Fe^{II}, Co^{II} and Ni^{II}) unit. The computed single-ion anisotropy values for the Fe^{II}, Co^{II} and Ni^{II} mononuclear units are given in Table 2. The axial zfs parameter D is estimated to be +20.17 cm^{-1}, +134.3 cm^{-1} and −0.02 cm^{-1} for Fe^{II}, Co^{II} and Ni^{II} mononuclear units respectively. The Ni^{II} ion zfs is computed to be very small and thus can be treated as an isotropic system similar to the Mn^{II} and Cu^{II} ions present in complexes **1** and **5**. Thus only the nature of single-ion anisotropy of the Fe^{II} and Co^{II} ions is discussed here. To rationalize the observed sign and magnitude of the D values, eigenvalue plots of the respective monomeric units were analysed (see Fig. 9).

The Fe^{II} ion has the following orbital ordering $(d_{yz})^2(d_{xy})^1(d_{xz})^1(d_{x^2-y^2})^1(d_{z^2})^1$ with a very small d_{yz}–d_{xy} energy gap and a significantly larger d_{yz}–d_{xz} gap. A very strong π-donor –CN ligand on the axial position stabilizes the d_{yz} orbitals compared to other orbitals. The DMF present in the equatorial position also acts as a π-acceptor ligand leading to the stabilization of d_{xy} orbitals. The π-interaction of the –CN ligand with the d_{xz} orbitals on the other hand is significantly less and this may be attributed to the acute M–N–C angle. This leads to the destabilization of these orbitals both in Fe^{II} and Co^{II} complexes. This orbital ordering has the following consequences for the Fe^{II} ion D value (i) the β electron from the d_{yz} to d_{xy} orbital has a very small transition energy and this is a spin-allowed transition between different $|\pm m_l|$ levels and thus contributes to positive D values. (ii) As the gap between the d_{yz} and d_{xz} orbital is significantly large, the negative contribution to the D value due to the $d_{yz} \rightarrow d_{xz}$ spin-allowed transition is small (transition between the same $|\pm m_l|$ levels) leading to an overall positive D value for the Fe^{II} mononuclear unit. For the Co^{II} complex, the $(d_{yz})^2(d_{xy})^2(d_{xz})^1(d_{x^2-y^2})^1(d_{z^2})^1$ configuration is noted and here $d_{xy} \rightarrow d_{xz}$ is expected to be dominant as the gap between these two orbitals is very small. This leads to a very large positive D value for this complex. The orientation of the D_{ZZ} axis of the Fe^{II} and Co^{II} ions along with the Re^{IV} ion anisotropy direction is shown in Fig. 10. The D_{zz} axis of the Fe^{II} and Co^{II} anisotropy is found to be tilted by 42.3° and 46.7° respectively, compared to the Re^{IV} D_{ZZ} axis. This is likely to significantly reduce the overall anisotropy of the building unit. Besides, the coupling with the Re^{IV} ion is likely to reduce the anisotropy of the building unit.[60] For example, although the Co^{II} ion has a significant single-ion anisotropy, only $1/5^{th}$ of that magnitude contributes to the overall anisotropy of the $S = 3$ spin coupled state of the $\{Re^{IV}$–$Co^{II}\}$ building unit (see the ESI† for further details). All these components put together substantially reduces the barrier height for magnetization reversal observed in this series.[12,60]

Table 2 CASSCF computed D and E values of complexes **2–4**

	Fe^{II} in complex **2**	Co^{II} in complex **3**	Ni^{II} in complex **4**
D	+20.17 cm^{-1}	+134.3 cm^{-1}	−0.02 cm^{-1}
E	−3.39 cm^{-1}	−29.6 cm^{-1}	0.01 cm^{-1}

Conclusions

In the present contribution we have studied in detail the mechanism of magnetic exchange in five dinuclear $\{Re^{IV}$–$M^{II}\}$ complexes to determine the factors which control the magnetic exchange coupling. Our calculations reproduce the sign of J values in all the cases studied. While the magnitude of J values is in agreement with experiments for $\{Re^{IV}$–$Mn^{II}\}$, $\{Re^{IV}$–$Ni^{II}\}$ and $\{Re^{IV}$–$Cu^{II}\}$ complexes some deviations are noted for $\{Re^{IV}$–$Fe^{II}\}$and $\{Re^{IV}$–$Co^{II}\}$complexes. A very large J value computed for the $\{Re^{IV}$–$Cu^{II}\}$ complex is in agreement with the record high ferromagnetic exchange reported for this complex. More importantly, we have established a mechanism of magnetic coupling for this series where five terms are found to contribute to the J values. Large and diffuse 5d orbitals of the Re^{IV} ion facilitate a strong magnetic exchange compared to their 3d analogues. The (Re)d_{yz}–d_{yz}(3d) overlap is found to be

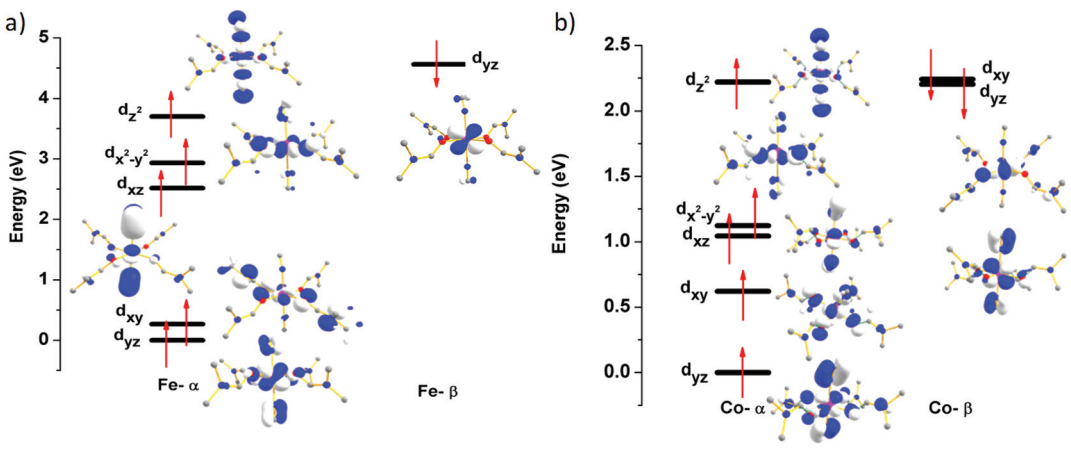

Fig. 9 Crystal field splitting pattern of d-orbitals of (a) Fe^{II} ion in complex **2**; (b) Co^{II} ion in complex **3** computed using DFT calculations. The iso-density surface of the orbital corresponds to a value of 0.036 e^- $bohr^{-3}$.

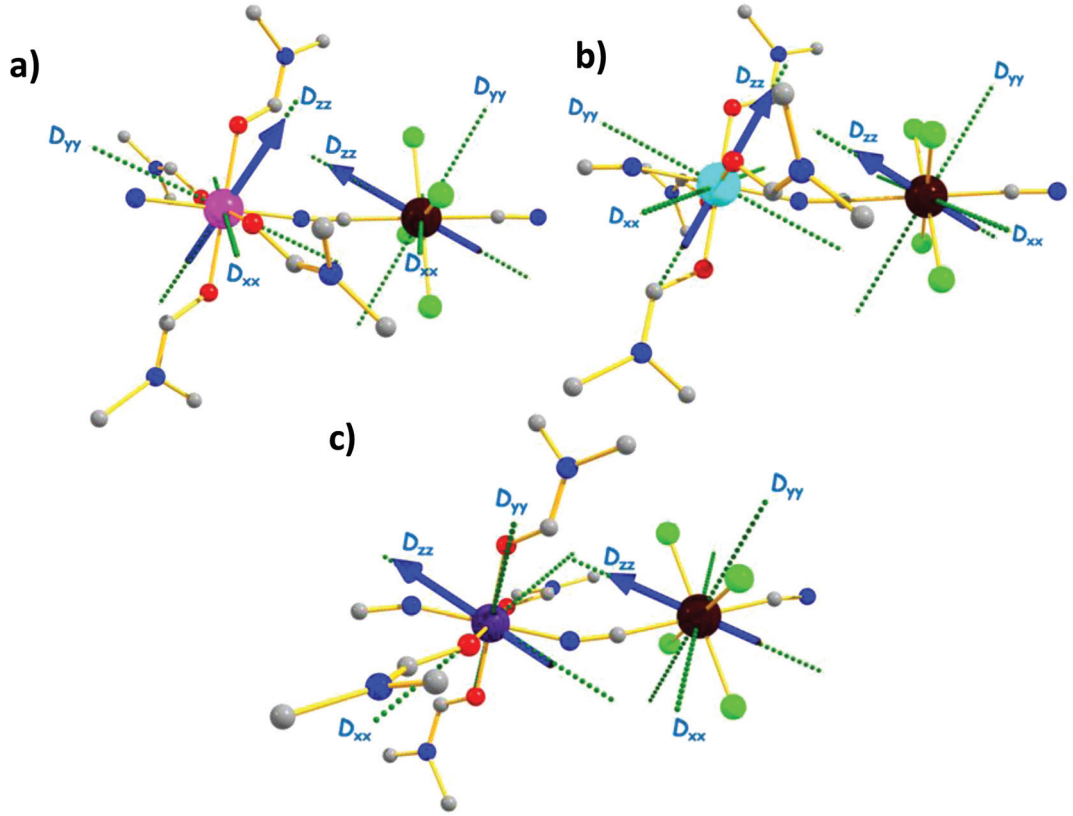

Fig. 10 Computed magnetic anisotropy directions for a dinuclear building unit in complexes (a) **2**; (b) **3** and (c) **4**.

significant and contributes to the antiferromagnetic part of the exchange while the equivalent (Re)d_{xz}–d_{xz}(3d) overlap is angle dependent and varies significantly with the variation in the M^{II}–N–C angle. The (Re)d_{xy}–d_{xy}(3d) overlap is found to contribute to the ferromagnetic coupling, while a significant orbital orthogonality between the t_{2g} orbital of the Re^{IV} ion and e_g-orbitals of M^{II} ions is noted, and this contributes to the ferromagnetic part of the exchange. Besides these interactions, cross interactions between the empty orbitals of the Re^{IV} ion and the occupied orbital of the M^{II} ions are noted, and this term is found to be dominant in the $\{Re^{IV}–Cu^{II}\}$ complex leading to a very large ferromagnetic J in this complex.

Magneto-structural correlations are developed for Re–C and M–N bond lengths and Re–C–N and M–N–C bond angles. Representative correlations developed for complexes **1** and **5** reveal a decrease in the magnitude of J values as the Re–C or M–N distances increase. The correlation developed for the M–N–C bond angle is found to be the most important parameter for all the complexes as it significantly alters the magnitude of J values and also found to switch the sign of J values at smaller angles. Particularly, the correlation developed for the Fe–N–C bond angle matches well with the experimental correlation developed earlier on a series of $\{Re^{IV}–Fe^{II}\}$ complexes. Most importantly, the mechanism of coupling established not only helps in rationalizing the trend observed among complexes **1–5**, but also rationalize the trend observed among the magneto-structural correlations developed.

Apart from the magnetic exchange interaction, we have also estimated the magnetic anisotropy of $[ReCl_4(CN)_2]^{2-}$ and $[(DMF)_4(CN)M^{II}(CN)]$ (M^{II}–Fe^{II}, Co^{II} and Ni^{II}) units by employing the state-of-the-art *ab initio* CASSCF/PT2/RASSI-SO/SINGLE_ANISO approach. The calculated D and E values are in agreement with the available experimental observations. A large positive D computed for the $[ReCl_4(CN)_2]^{2-}$ unit stems from the low-lying doublet states which corresponds to the excitation between different $|m_l|$ levels ($d_{xz}/d_{yz} \rightarrow d_{xy}$). Similarly large and very large positive D values computed for Fe^{II} and Co^{II} units corroborate with the small transition energy between different $|m_l|$ levels (for example $d_{yz} \rightarrow d_{xy}$) and ground state electronic configurations established. The non-collinearity of the Re^{IV} and M^{II} ions in the D_{ZZ} axis is found to diminish the anisotropy of the building unit, leading to the observation of moderate relaxation barriers/SCM behaviours in this series.

Acknowledgements

GR would like to thank DST (Grant EMR/2014/000247) Nano-Mission (SR/NM/NS-1119/2011) for the funding and IITB for generous high performance computing facility. SKS would like to thank the Department of Chemistry for Research Associate position. KRV would like to thank the IITB-Monash Academy for research funding. VA would like to thank IRCC for a summer project fellowship at IITB.

References

1 W. Wernsdorfer and R. Sessoli, *Science*, 1999, **284**, 133–135.
2 R. Sessoli, D. Gatteschi, A. Caneschi and M. A. Novak, *Nature*, 1993, **365**, 141–143.
3 L. Ungur, S. K. Langley, T. N. Hooper, B. Moubaraki, E. K. Brechin, K. S. Murray and L. F. Chibotaru, *J. Am. Chem. Soc.*, 2012, **134**, 18554–18557.
4 A. Prescimone, J. Wolowska, G. Rajaraman, S. Parsons, W. Wernsdorfer, M. Murugesu, G. Christou, S. Piligkos, E. J. L. McInnes and E. K. Brechin, *Dalton Trans.*, 2007, 5282–5289, DOI: 10.1039/b713163a.
5 C. J. Milios, M. Manoli, G. Rajaraman, A. Mishra, L. E. Budd, F. White, S. Parsons, W. Wernsdorfer, G. Christou and E. K. Brechin, *Inorg. Chem.*, 2006, **45**, 6782–6793.
6 R. Sessoli and A. K. Powell, *Coord. Chem. Rev.*, 2009, **253**, 2328–2341.
7 L. R. Piquer and E. C. Sanudo, *Dalton Trans.*, 2015, **44**, 8771–8780.
8 D. N. Woodruff, R. E. P. Winpenny and R. A. Layfield, *Chem. Rev.*, 2013, **113**, 5110–5148.
9 A. Ardavan, O. Rival, J. J. L. Morton, S. J. Blundell, A. M. Tyryshkin, G. A. Timco and R. E. P. Winpenny, *Phys. Rev. Lett.*, 2007, **98**, 057201.
10 G. Christou, D. Gatteschi, D. N. Hendrickson and R. Sessoli, *MRS Bull.*, 2000, **25**, 66–71.
11 O. Waldmann, *Inorg. Chem.*, 2007, **46**, 10035–10037.
12 S. K. Singh and G. Rajaraman, *Chem. – Eur. J.*, 2014, **20**, 5214–5218.
13 D. E. Freedman, W. H. Harman, T. D. Harris, G. J. Long, C. J. Chang and J. R. Long, *J. Am. Chem. Soc.*, 2010, **132**, 1224–1225.
14 J. M. Zadrozny, J. Telser and J. R. Long, *Polyhedron*, 2013, **64**, 209–217.
15 R. A. A. Cassaro, S. G. Reis, T. S. Araujo, P. M. Lahti, M. A. Novak and M. G. F. Vaz, *Inorg. Chem.*, 2015, **54**, 9381–9383.
16 F. Pointillart, K. Bernot, G. Poneti and R. Sessoli, *Inorg. Chem.*, 2012, **51**, 12218–12229.
17 L. Bogani, A. Vindigni, R. Sessoli and D. Gatteschi, *J. Mater. Chem.*, 2008, **18**, 4750–4758.
18 T. D. Harris, M. V. Bennett, R. Clérac and J. R. Long, *J. Am. Chem. Soc.*, 2010, **132**, 3980.
19 M. G. F. Vaz, R. A. A. Cassaro, H. Akpinar, J. A. Schlueter, P. M. Lahti and M. A. Novak, *Chem. – Eur. J.*, 2014, **20**, 5460–5467.
20 K. Bernot, L. Bogani, A. Caneschi, D. Gatteschi and R. Sessoli, *J. Am. Chem. Soc.*, 2006, **128**, 7947–7956.
21 W.-X. Zhang, R. Ishikawa, B. Breedlove and M. Yamashita, *RSC Adv.*, 2013, **3**, 3772–3798.
22 K. Bernot, J. Luzon, R. Sessoli, A. Vindigni, J. Thion, S. Richeter, D. Leclercq, J. Larionova and A. van der Lee, *J. Am. Chem. Soc.*, 2008, **130**, 1619.
23 X. Y. Wang, C. Avendano and K. R. Dunbar, *Chem. Soc. Rev.*, 2011, **40**, 3213–3238.
24 A. Palii, B. Tsukerblat, S. Klokishner, K. R. Dunbar, J. M. Clemente-Juan and E. Coronado, *Chem. Soc. Rev.*, 2011, **40**, 3130–3156.
25 V. S. Mironov, *J. Magn. Magn. Mater.*, 2004, **272**, E731–E733.
26 V. S. Mironov, L. F. Chibotaru and A. Ceulemans, *J. Am. Chem. Soc.*, 2003, **125**, 9750–9760.
27 J. Dreiser, K. S. Pedersen, A. Schnegg, K. Holldack, J. Nehrkorn, M. Sigrist, P. Tregenna-Piggott, H. Mutka, H. Weihe, V. S. Mironov, J. Bendix and O. Waldmann, *Chem. – Eur. J.*, 2013, **19**, 3693–3701.
28 S. K. Singh and G. Rajaraman, *Chem. – Eur. J.*, 2014, **20**, 113–123.
29 M. Atanasov, P. Comba, S. Hausberg and B. Martin, *Coord. Chem. Rev.*, 2009, **253**, 2306–2314.
30 M. Atanasov, P. Comba and C. A. Daul, *Inorg. Chem.*, 2008, **47**, 2449–2463.
31 T. D. Harris, M. V. Bennett, R. Clerac and J. R. Long, *J. Am. Chem. Soc.*, 2010, **132**, 3980–3988.
32 X. W. Feng, J. J. Liu, T. D. Harris, S. Hill and J. R. Long, *J. Am. Chem. Soc.*, 2012, **134**, 7521–7529.
33 D. E. Freedman, D. M. Jenkins, A. T. Iavarone and J. R. Long, *J. Am. Chem. Soc.*, 2008, **130**, 2884–2885.
34 K. S. Pedersen, M. Schau-Magnussen, J. Bendix, H. Weihe, A. V. Palii, S. I. Klokishner, S. Ostrovsky, O. S. Reu, H. Mutka and P. L. W. Tregenna-Piggott, *Chem. – Eur. J.*, 2010, **16**, 13458–13464.
35 K. S. Pedersen, J. Dreiser, J. Nehrkorn, M. Gysler, M. Schau-Magnussen, A. Schnegg, K. Holldack, R. Bittl, S. Piligkos, H. Weihe, P. Tregenna-Piggott, O. Waldmann and J. Bendix, *Chem. Commun.*, 2011, **47**, 6918–6920.
36 X. W. Feng, T. D. Harris and J. R. Long, *Chem. Sci.*, 2011, **2**, 1688–1694.
37 T. D. Harris, C. Coulon, R. Clerac and J. R. Long, *J. Am. Chem. Soc.*, 2011, **133**, 123–130.
38 M. Atanasov, C. Busche, P. Comba, H. F. El, B. Martin, G. Rajaraman, S. J. van and H. Wadepohl, *Inorg. Chem.*, 2008, **47**, 8112–8125.
39 J. Dreiser, A. Schnegg, K. Holldack, K. S. Pedersen, M. Schau-Magnussen, J. Nehrkorn, P. Tregenna-Piggott, H. Mutka, H. Weihe, J. Bendix and O. Waldmann, *Chem. – Eur. J.*, 2011, **17**, 7492–7498.
40 E. Ruiz, G. Rajaraman, S. Alvarez, B. Gillon, J. Stride, R. Clerac, J. Larionova and S. Decurtins, *Angew. Chem., Int. Ed.*, 2005, **44**, 2711–2715.
41 E. Ruiz, S. Alvarez, A. Rodriguez-Fortea, P. Alemany, Y. Pouillon and C. Massobrio, in *Magnetism: Molecules to Materials II: Molecule-Based Materials*, ed. J. S. Miller and M. Drillon, Wiley-VCH Verlag GmbH & Co. KGaA, Weinheim, 2001, vol. 110, ch. 7, pp. 227–280.
42 L. Noodleman, *J. Chem. Phys.*, 1981, **74**, 5737–5743.
43 K. Yamaguchi, F. Jensen, A. Dorigo and K. N. Houk, *Chem. Phys. Lett.*, 1988, **149**, 537–542.
44 T. Soda, Y. Kitagawa, T. Onishi, Y. Takano, Y. Shigeta, H. Nagao, Y. Yoshioka and K. Yamaguchi, *Chem. Phys. Lett.*, 2000, **319**, 223–230.

45 K. Yamaguchi, Y. Takahara and T. Fueno, *Applied Quantum Chemistry*, Reidel, Dordrecht, 1986, 155.
46 E. Ruiz, J. Cano, S. Alvarez and P. Alemany, *J. Comput. Chem.*, 1999, **20**, 1391–1400.
47 S. K. Singh, N. K. Tibrewal and G. Rajaraman, *Dalton Trans.*, 2011, **40**, 10897–10906.
48 M. J. Frisch, G. W. Trucks, H. B. Schlegel, G. E. Scuseria, M. A. Robb, J. R. Cheeseman, G. Scalmani, V. Barone, B. Mennucci, G. A. Petersson, H. Nakatsuji, M. Caricato, X. Li, H. P. Hratchian, A. F. Izmaylov, J. Bloino, G. Zheng, J. L. Sonnenberg, M. Hada, M. Ehara, K. Toyota, R. Fukuda, J. Hasegawa, M. Ishida, T. Nakajima, Y. Honda, O. Kitao, H. Nakai, T. Vreven, J. A. Montgomery Jr., J. E. Peralta, F. Ogliaro, M. J. Bearpark, J. Heyd, E. N. Brothers, K. N. Kudin, V. N. Staroverov, R. Kobayashi, J. Normand, K. Raghavachari, A. P. Rendell, J. C. Burant, S. S. Iyengar, J. Tomasi, M. Cossi, N. Rega, N. J. Millam, M. Klene, J. E. Knox, J. B. Cross, V. Bakken, C. Adamo, J. Jaramillo, R. Gomperts, R. E. Stratmann, O. Yazyev, A. J. Austin, R. Cammi, C. Pomelli, J. W. Ochterski, R. L. Martin, K. Morokuma, V. G. Zakrzewski, G. A. Voth, P. Salvador, J. J. Dannenberg, S. Dapprich, A. D. Daniels, Ö. Farkas, J. B. Foresman, J. V. Ortiz, J. Cioslowski and D. J. Fox, *Gaussian 09 (Revision A.02)*, 2009.
49 F. Weigend and R. Ahlrichs, *Phys. Chem. Chem. Phys.*, 2005, **7**, 3297–3305.
50 F. Aquilante, T. B. Pedersen, V. Veryazov and R. Lindh, *Wiley Interdiscipl. Rev.: Comput. Mol. Sci.*, 2013, **3**, 143–149.
51 L. Chibotaru and L. Ungur, *The computer programs SINGLE_ANISO and POLY_ANISO*, University of Leuven, 2006.
52 L. Ungur and L. Chibotaru, *Lanthanides and Actinides in Molecular Magnetism*, Wiley-VCH Verlag GmbH & Co. KGaA, New York, 2015.
53 D. Pinkowicz, H. Southerland, X. Y. Wang and K. R. Dunbar, *J. Am. Chem. Soc.*, 2014, **136**, 9922–9924.
54 Z. J. Zhong, N. Matsumoto, H. Okawa and S. Kida, *Inorg. Chem.*, 1991, **30**, 436–439.
55 K. Wieghardt, U. Bossek, D. Ventur and J. Weiss, *J. Chem. Soc., Chem. Commun.*, 1985, 347–349, DOI: 10.1039/c39850000347.
56 N. Berg, T. Rajeshkumar, S. M. Taylor, E. K. Brechin, G. Rajaraman and L. F. Jones, *Chem. – Eur. J.*, 2012, **18**, 5906–5918.
57 E. Ruiz, J. Cirera and S. Alvarez, *Coord. Chem. Rev.*, 2005, **249**, 2649–2660.
58 S. K. Singh, T. Rajeshkumar, V. Chandrasekhar and G. Rajaraman, *Polyhedron*, 2013, **66**, 81–86.
59 S. K. Singh and G. Rajaraman, *Nat. Commun.*, 2016, **7**, 10669.
60 A. Bencini and D. Gatteschi, *Electron Paramagnetic Resonance of Exchange Coupled Systems*, Springer, 2011.

